



ELSEVIER

Available online at www.sciencedirect.com

SCIENCE @ DIRECT®

Journal of Magnetism and Magnetic Materials 267 (2003) 92–96

Journal of
magnetism
and
magnetic
materials

www.elsevier.com/locate/jmmm

Mössbauer identification of μ -type metastable phase as the main magnetic component in $\text{Nd}_{60}\text{Fe}_{30}\text{Al}_{10}$ melt spun alloys

C.E. Rodríguez Torres^{a,c}, A.F. Cabrera^{a,c}, F.H. Sánchez^{a,c}, O.V. Billoni^{b,c},
S.E. Urreta^{b,*}, L.M. Fabietti^{b,c}

^a *Facultad de Ciencias Exactas, Universidad Nacional de La Plata, 1900 La Plata, Argentina*

^b *Facultad de Matemática Astronomía y Física, Universidad Nacional de Córdoba, Ciudad Universitaria FAMAF,
5000 Córdoba, Argentina*

^c *CONICET Argentina*

Received 20 February 2003; received in revised form 4 April 2003

Abstract

The local atomic arrangements and the nanoscopically dispersed phases in melt spun $\text{Nd}_{60}\text{Fe}_{30}\text{Al}_{10}$ alloys are investigated by Mössbauer spectroscopy. It is found that the hard magnetic properties of these alloys are likely to be related to the presence of clusters of a metastable crystalline μ -type phase.

© 2003 Elsevier Science B.V. All rights reserved.

PACS: 75.50.Kj

Keywords: Amorphous RE-TM alloys; Mössbauer Spectroscopy; Hard magnetic properties

1. Introduction

Magnetic amorphous materials based on rare-earth and transition metals have been intensively studied because of their interesting physical properties and potential applications; they are suitable for magnetic recorder media, permanent magnets and magneto-optical and magneto-strictive devices. Despite these studies, however, the temperature dependence of the magnetic properties of melt spun $\text{Nd}_{60}\text{Fe}_{30}\text{Al}_{10}$ alloys, and their

relation with the microstructure or quenching rate are still not well explained. As a function of temperature, the magnetization and the hysteresis loops exhibit complex multi-magnetic phase behaviors which are strongly sensitive to the quenching rate [1–5]. The hard magnetic properties of these alloys are related to a nominally amorphous ferromagnetic matrix, in which small paramagnetic particles are dispersed. A better understanding of the atomic microstructure of this ferromagnetic component and its influence on the magnetic microstructures and coercivity becomes necessary for further improvement of the magnetic properties.

Recent research works have shown that the ferromagnetic matrix contains a high density of

*Corresponding author. Tel.: +54-451-433-4051; fax: +54-451-433-4054.

E-mail address: urreta@mail.famaf.unc.edu.ar
(S.E. Urreta).

Fe-rich clusters, embedded in a Nd-rich amorphous phase. The hard magnetic properties were suggested to be due to exchange coupling interactions between these clusters (with a large, random magnetic anisotropy) [6]. The structural and magnetic characterization of the Fe-rich phase, however, remains open. While Kramer et al. [7] suggest that these clusters are likely to be chemically and structurally related to the δ -phase ($\text{Nd}_6\text{Fe}_{13-x}\text{Al}_{1+x}$) other authors claim that they are agglomerates of atoms without any ordered arrangement, i.e. amorphous clusters [8,9].

In this letter, we report our recent Mössbauer effect (ME) spectroscopy results in melt spun $\text{Nd}_{60}\text{Fe}_{30}\text{Al}_{10}$ alloys, quenched at different rates, from which the Fe-rich clusters phase could be quantified and identified as the metastable μ phase [10]. This represents an important advance in the understanding of the magnetic properties of Nd–Fe–Al alloys which may be used to improve the theoretical simulation of their magnetic behavior. The presence of these clusters could also be correlated with the hard magnetic properties observed at room temperature.

2. Experimental procedures

The alloy, prepared by arc melting 99.9% Nd, 99.9% Fe and 99.99% Al, was further processed by melt spinning onto a single copper wheel at tangential speeds of 5 and 20 m/s to obtain samples V5 and V20, respectively. Mössbauer spectra were recorded in transmission geometry using a constant acceleration spectrometer with a 10-mCi $^{57}\text{CoRh}$ source at room temperature and at 85 K. The hysteresis loops for a maximum field of 1.5 T were measured at room temperature, using a field rate $R = 2 \text{ T/min}$. The reversible susceptibility $\chi_{\text{rev}}(H_i)$ was estimated as the mean slope of a small recoil loop traced after a waiting time of 100 s at different inverse fields; the irreversible susceptibility was then approximated by $\chi_{\text{irr}}(H_i) = \chi_{\text{T}}(H_i) - \chi_{\text{rev}}(H_i)$, with the total susceptibility χ_{T} determined by differentiation of the total polarization J on the major loop with respect to the internal field $\mu_0 H_i$.

3. Results and discussion

The XRD patterns resulted similar to those previously reported [4,7]; they show halos, typical of an amorphous structure, along with crystalline peaks corresponding to the hexagonal Nd phase (present in both samples, but with a more pronounced crystallinity in the slowly cooled ribbons).

Fig. 1 shows the room temperature (RT) and 85 K ME spectra of ribbons melt-spun at 5 m/s. The RT spectrum has similar features to those reported by Wang et al. [4]. Although they propose the existence of a large amorphous contribution, the need of at least three magnetic Voigtian components plus two non-magnetic ones for spectral analysis suggests the presence of important crystalline-like contributions. Visual comparison strongly suggests interesting similarities with the Mössbauer spectrum reported by Politano et al. [10] for the pure μ phase. These similarities were further supported by the quantitative analysis of the spectra of Fig. 1 (see below).

The μ -phase is the stable ternary phase with the lowest amount of aluminum ($\text{Nd}_{33.3}\text{Fe}_{66.7-x}\text{Al}_x$,

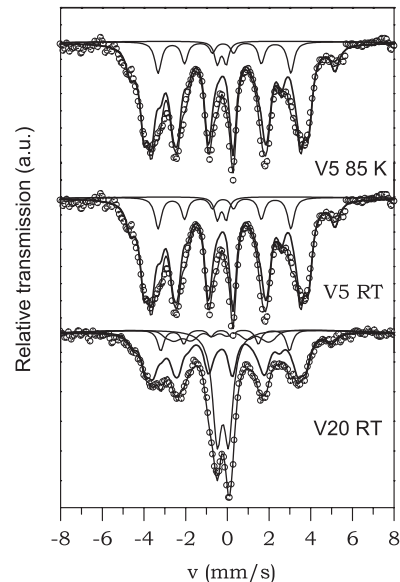


Fig. 1. Mössbauer spectra of ribbons melt-spun at 5 m/s (85 K and RT) and 20 m/s (RT), showing the subspectrum of the μ -type phase.

$2.5 < x < 5$) and a rather complex crystalline structure. TEM investigations reveal that the μ phase consists of a long-period stacking of planes, typical of polytypism, each plane being constituted by a hexagonal array of structural units [11]; due to this structure, this phase exhibits a complex XRD pattern, hardly distinguishable even in almost single-phase samples. The μ phase is ferromagnetic, with a large anisotropy field $\mu_0 H_A > 8$ T, a saturation magnetization of 0.85 T [12] and a Curie temperature in the range 510–533 K [10]. It is closely related to the metastable Al phase responsible for the large room temperature coercivities of $\text{Nd}_{100-x}\text{Fe}_x$ ($30 < x < 60$).

In order to make a more quantitative assessment, the spectrum was fitted using a practical method of fitting complex multiphase ME spectra [13]. This routine describes each multisite phase using only four parameters: relative area (A), elemental linewidth (Γ), mean isomer shift (δ) and mean hyperfine field (B). Both spectra (RT and 85 K) were fitted with three components: a simulated multisite spectrum of the μ -phase ($\text{Nd}_{37}\text{Fe}_{58}\text{Al}_5$) [14], one magnetic sextet and a non magnetic doublet. The fitted parameters were: the relative fraction of the three components, the average isomer shift and the hyperfine field of the simulated component, and the hyperfine parameters of the sextet and the doublet. With this procedure the main spectral characteristics were well reproduced, the contribution of the μ -phase being apparent. The paramagnetic component is tentatively ascribed to a small amount of Fe ($\approx 3\%$) dissolved in the Nd-rich amorphous phase while the origin of the sextet ($\approx 10\%$ of Fe) remains uncertain. The best-fit parameters are listed in Table 1.

Although our spectra strongly resemble the pattern of that of the μ -phase, the average hyperfine field is about 9% lower. This may indicate that our samples are slightly enriched in Al (and consequently rarified in Fe) as compared to the stoichiometric μ -phase. For $\text{Nd}_{60}\text{Fe}_{30}\text{Al}_{10}$ the equilibrium phase diagram predicts the formation of a paramagnetic δ -phase, $\text{Nd}_{30}\text{Fe}_{70-x}\text{Al}_x$ ($8 < x < 25$), with an Al concentration larger than that reported for the μ -phase [12]. We conclude that the non-equilibrium preparation route pre-

Table 1

Fitted parameters (average hyperfine field B , isomer shift δ , quadrupolar shift ε (magnetic sextet), quadrupolar splitting Δ (paramagnetic doublet), relative intensity A) of V5 and V20

Sample	Identification	B^a (T)	δ^a (mm/s)	ε/Δ (mm/s)	A (%)
V5 (RT)	μ -type phase	23.5	−0.07	—	87
	Unidentified	19.8	−0.08	0.04	10
	Nd-rich phase	—	−0.16	0.43	3
V5 (85 K)	μ -type phase	26.9	0.02	—	86
	Unidentified	22.9	0.02	0.04	11
	Nd-rich phase	—	−0.001	0.44	3
V20 (RT)	μ -type phase	22.8	−0.09	—	54
	Unidentified	19.2	−0.10	0.09	8
	Nd-rich phase	—	−0.11	0.55	28
	HFD	14.7	−0.22	0.03	10

Values of δ are relative to α -Fe. Errors for hyperfine parameters are ± 0.1 T for B and ± 0.01 mm/s for δ , ε and Δ .

^a Mean values in the cases of the HFD and the μ -type phase.

vents the formation of the δ -phase, giving rise to a metastable μ -phase with higher Al content.

Detailed XRD, TEM and SAD investigation carried out on mold cast samples of $\text{Nd}_{60}\text{Fe}_x\text{Co}_{30-x}\text{Al}_{10}$ ($x > 10$) by Kumar et al. [9], revealed the existence of Fe-rich regions in which layers about 50 nm thick of a metastable U-phase (μ -type) formed. These authors did not detect U-phase in melt spun ribbons (cooled at a much higher rate) but they observed that these specimens exhibited thermomagnetic curves similar to the mold cast samples. This behavior suggests that the metastable U-phase could be present in the ribbons but with such small microstructure that neither XRD nor their TEM or SAD observations could resolve its characteristic signatures (Fe rich clusters would be about 2 nm in size). One distinguishing feature of ME spectroscopy is its ability for sensing the surrounding of a given probe (in our case ^{57}Fe), which allows short-range ordered structures to be detected. This unique ability permits the detection and identification of nanoscopically dispersed phases and local atomic arrangements.

The ME spectrum of the ribbon melt-spun at 20 m/s (see Fig. 1 and Table 1) was fitted with the same components of the V5 plus a magnetic hyperfine field distribution (HFD). The amount

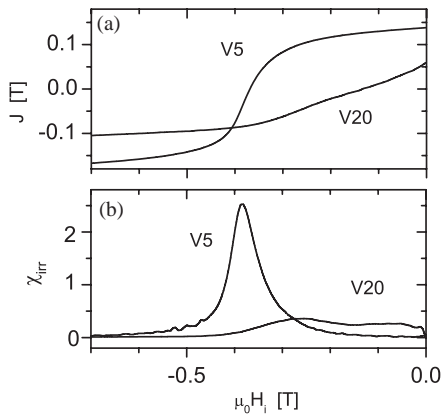


Fig. 2. Demagnetization (a) and irreversible susceptibility χ_{irr} (b) curves for specimens V5 and V20; $R = 2 \text{ T/min}$, $T = 300 \text{ K}$.

of Fe in the magnetic μ phase-like component decreased (86–54%) in the benefit of the paramagnetic component and of a new magnetic contribution, introduced in order to account for the larger depth of the 2 and 5 absorption lines. This corresponds to a hyperfine field distribution which reflects the increase of iron atoms in the amorphous Nd-rich phase whose formation was favored by the higher cooling rate.

The demagnetization and irreversible susceptibility curves for V5 and V20 are shown in Fig. 2. V20 exhibits two small, broad peaks in χ_{irr} and a relatively large reversible susceptibility near $H_i = 0$. This indicates that magnetically hard and soft regions coexist in the sample, reversing their polarization quite independently (weak coupling regime). This hysteresis behavior is then compatible with the multi-phase microstructure deduced from ME, in which crystalline and amorphous magnetic phases are found to coexist.

The irreversible susceptibility in V5 shows a large, relatively narrow peak at a higher inverse field (with small values of χ_{rev} at low fields) indicating that the sample behaves as a hard single-magnetic phase system. The volume fraction of the ferromagnetic phase is reported to increase [5] as the quenching rate decreases; this fact and our ME and hysteresis results may be conciliated by considering: (a) quenching at lower rates increases the volume fraction of μ -type clusters at expenses of the surrounding (ferro and paramagnetic)

amorphous phases, and (b) these μ clusters confere the hard magnetic properties to the alloy.

4. Conclusions

Melt spun $\text{Nd}_{60}\text{Fe}_{30}\text{Al}_{10}$ alloys have been studied by Mössbauer Effect spectroscopy in the as quenched condition. While XRD results show only the presence of dhcp-Nd and an amorphous phase, ME allows to detect ^{57}Fe probes in three different environments: one of them is identified as Fe in a Nd-rich amorphous phase (paramagnetic), another one is Fe in an unidentified phase (magnetic) and the third one, giving the main contribution to the spectrum, is the metastable μ -type phase. As the quenching rate increases from 5 to 20 m/s, the amount of this metastable, magnetically hard phase is found to decrease, while the amounts of Fe-rich and Nd-rich amorphous phases increase; at the same time, the hysteresis loop changes from one characteristic of a hard, single-magnetic phase system to a two-step loop, associated to the coexistence of weakly coupled hard and soft phases.

Acknowledgements

This work has been partially supported by SECyT-UNC, ACC S.E. and CONICET Argentina.

References

- [1] G. Kumar, J. Eckert, S. Roth, K.H. Müller, L. Schultz, J. Alloys Compounds 348 (2003) 309.
- [2] D. Triyono, R. Sato Turtelli, R. Grössinger, H. Michor, K.R. Pirota, M. Knobel, H. Sassik, T. Mathias, S. Höfingler, J. Fidler, J. Magn. Magn. Mater. 242–245 (2002) 1321.
- [3] B.C. Wei, W. Lösser, L. Xia, S. Roth, M.X. Pan, W.H. Wang, J. Eckert, Acta Mater. 50 (2002) 4357.
- [4] L. Wang, J. Ding, Y. Li, Y.P. Feng, X.Z. Wang, N.X. Phuc, N.H. Dan, J. Magn. Magn. Mater. 224 (2001) 143.
- [5] N.H. Dan, N.X. Phuc, N.M. Hong, J. Ding, D. Givord, J. Magn. Magn. Mater. 226–230 (2001) 1385.
- [6] L. Wang, J. Ding, H.Z. Kong, Y. Li, Y.P. Feng, Phys. Rev. B 64 (2001) 214410.

- [7] M.J. Kramer, A.S. O'Connor, K.W. Dennis, R.W. McCallum, L.H. Lewis, L.D. Tung, N.P. Duong, *IEEE Trans. on Magn.* 37 (4) (2001) 2497.
- [8] H.Z. Kong, J. Ding, Z.L. Dong, L. Wang, T. White, Y. Li, *J. Phys. D* 35 (2002) 423.
- [9] G. Kumar, J. Eckert, S. Roth, W. Lösser, L. Schultz, S. Ram, *Acta Mater.* 51 (2003) 229.
- [10] R. Politano, A.C. Neiva, H.R. Rechenberg, F.P. Missell, *J. Alloys Compounds*. 184 (1992) 121.
- [11] J. Delamare, D. Lamarchand, P. Vigier, *J. Magn. Magn. Mater.* 104–107 (1992) 1092.
- [12] B. Grieb, E.-Th. Henig, G. Martinek, H.H. Stadelmaier, G. Petzow, *IEEE Trans. on Magn.* 26 (5) (1990) 1367.
- [13] F.H. Sánchez, C.E. Rodríguez Torres, F.D. Saccone, A. Ayala, *Hyperfine Interactions* 33 (2001) 133.
- [14] J.M. Le Breton, J. Teillet, D. Lemarchand, V. de Pauw, *J. Alloys Compounds* 218 (1995) 31.